2012

An Extracellular Domain of the Accessory Beta1 Subunit Is Required for Modulating BK Channel Voltage Sensor and Gate

Aleksandra Gruslova

Iurii Semenov
Old Dominion University, isemenov@odu.edu

Bin Wang

An extracellular domain of the accessory β1 subunit is required for modulating BK channel voltage sensor and gate

Aleksandra Gruslova, Iurii Semenov, and Bin Wang

Department of Physiology, The University of Texas Health Science Center at San Antonio, San Antonio, TX 78229

A family of tissue-specific auxiliary β subunits modulates large conductance voltage- and calcium-activated potassium (BK) channel gating properties to suit their diverse functions. Paradoxically, β subunits both promote BK channel activation through a stabilization of voltage sensor activation and reduce BK channel openings through an increased energetic barrier of the closed-to-open transition. The molecular determinants underlying β subunit function, including the dual gating effects, remain unknown. In this study, we report the first identification of a β1 functional domain consisting of Y74, S104, Y105, and I106 residues located in the extracellular loop of β1. These amino acids reside within two regions of highest conservation among related β1, β2, and β4 subunits. Analysis in the context of the Horrigan-Aldrich gating model revealed that this domain functions to both promote voltage sensor activation and also reduce intrinsic gating. Free energy calculations suggest that the dual effects of the β1 Y74 and S104–I106 domains can be largely accounted for by a relative destabilization of channels in open states that have few voltage sensors activated. These results suggest a unique and novel mechanism for β subunit modulation of voltage-gated potassium channels wherein interactions between extracellular β subunit residues with the external portions of the gate and voltage sensor regulate channel opening.

INTRODUCTION

BK channels have an established role in regulating vascular smooth muscle tone by hyperpolarizing the membrane and deactivating voltage-dependent Ca^{2+} channels (Kaczorowski et al., 1996; Gribkoff et al., 1997; Calderone, 2002). Increased opening of smooth muscle BK channels is conferred by the β1 auxiliary subunit (Tanaka et al., 1997; Brenner et al., 2000b; Plüger et al., 2000). The important role of the β1 subunit has been demonstrated in β1 knockout mice, which display reduced BK channel opening, increased vascular tone, and hypertension (Brenner et al., 2000b; Plüger et al., 2000). In addition, two human β1 polymorphisms, each with a single amino acid change in the extracellular domain, have been associated with altered smooth muscle function. A gain-of-function polymorphism has been linked to a reduced incidence of hypertension (Fernández-Fernández et al., 2004). In addition, a polymorphism that moderately reduces channel opening has been associated with increased asthma severity (Seibold et al., 2008).

The BK channel pore-forming α subunit belongs to the six-transmembrane (TM) voltage-dependent K^+ channel family (Atkinson et al., 1991). The β1 accessory subunit belongs to the two-TM BK channel auxiliary β subunit family consisting of four members, β1–β4, each having distinct tissue-specific expression (Knaus et al., 1994; Riazi et al., 1999; Wallner et al., 1999; Xia et al., 1999;

Behrens et al., 2000; Brenner et al., 2000a). The β subunit structure contains a large extracellular loop, two TMs, and two small intracellular domains (Knaus et al., 1994; Orio et al., 2002). Recently, a distinct single TM protein, LRRC26 (leucine-rich repeat–containing protein 26), was also found to act as an accessory BK channel subunit in a prostate cancer cell line (Yan and Aldrich, 2010).

Mutagenesis of the α subunit has yielded a large number of insights into the structure of the pore-forming subunit of the BK channel (Lee and Cui, 2010). In contrast, the β structural determinants that modulate α subunit gating remain unclear. BK channel β subunits are apparently unrelated to other protein families. Therefore, identifying structural domains of β subunits by scanning mutagenesis is encumbered by the potentially large number of mutations that would be required. However, there is evidence that some modulatory effects of β subunit family members β1, β2, and β4 are conserved. These β subunits slow activation and deactivation gating kinetics (Behrens et al., 2000; Brenner et al., 2000a; Lippiat et al., 2003). In addition, these β subunits exert similar Ca^{2+}-dependent effects on steady-state opening (Behrens et al., 2000; Brenner et al., 2000a; Lippiat et al., 2003). They increase channel opening in high Ca^{2+}, effects that are accounted for by

Correspondence to Bin Wang: wangb3@uthscsa.edu

Abbreviation used in this paper: TM, transmembrane.

The Rockefeller University Press $30.00
J. Gen. Physiol. Vol. 139 No. 1   57–67
www.jgp.org/cgi/doi/10.1085/jgp.201110698

57

β subunit modulation of voltage sensor and Ca²⁺ binding (Bao and Cox, 2005; Orio and Latorre, 2005; Wang and Brenner, 2006; Wang et al., 2006; Sweet and Cox, 2009). β subunits also reduce channel opening in low intracellular Ca²⁺ by a reduction of intrinsic gating (channel opening independent of voltage sensor activation and Ca²⁺ binding; Orio and Latorre, 2005; Wang and Brenner, 2006; Wang et al., 2006). These functional similarities suggest that structural determinants underlying β subunit function may also be conserved (Orio et al., 2006). Therefore, key residues and functional domains may be uncovered by alanine substitution of conserved amino acids. Using this approach, we report here the identification of a novel β1 extracellular domain that is critical for modulation of voltage sensor activation and intrinsic gating of BK channels.

MATERIALS AND METHODS

Channel expression
The mouse BK α cDNA (GenBank/EMBL/DDBJ accession no. MMU09383) was modified to include the extended amino-terminal sequence (beginning MANG) encoded by the *KCNMA1* gene. We found that the extra sequence causes an ∼20-mV larger negative G-V shift by mouse β1 as compared with the truncated α subunit (initiating translation at the internal MDAL residues) that has been most often used in the past. The extended amino-terminal sequence was also added to the F315Y construct (Wang and Brenner, 2006), which we call F380Y in this study. With mouse β1 cDNA (Wang and Brenner, 2006) as a template, mutant β1 constructs were generated with a Quick-Change XL Site-Directed Mutagenesis kit (Agilent Technologies) and confirmed by sequencing.

α and various β1 cDNAs were cotransfected into HEK-293 cells (American Type Culture Collection) and studied 1–2 d after transfection. β1 subunits were subcloned in the mammalian expression vector pIRES2–enhanced green fluorescent protein (Takara Bio Inc.), which contains the enhanced green fluorescent protein gene that fluorescently labels transfected cells. A molar ratio of 1:6 α/β1 was used, aiming to saturate BK channels with β1 subunits. For β1 mutants with large effects on G-Vs, saturating β1 expression was experimentally verified (Fig. S2). In the event β1 expression did not reach saturation, reduced α/β1 molar ratios (1:12 and 1:24) were used to reach saturation.

Electrophysiology and data analysis
Currents were recorded using the patch clamp technique in the inside-out configuration. The external recording solution contained 20 mM HEPES, 140 mM KMeSO₃, 2 mM KCl, and 2 mM MgCl₂, pH 7.2. Internal solutions contained 20 mM HEPES, 140 mM KMeSO₃, and 2 mM KCl, pH 7.2. For the 60-µM free Ca²⁺ intracellular solution, Ca²⁺ was buffered with 5 mM nitrilo-triacetic acid. For nominally 0 Ca²⁺ (0.002 µM of free Ca²⁺), intracellular solution Ca²⁺ was buffered with 2 mM EGTA. Free [Ca²⁺] was measured using a Ca²⁺-sensitive electrode (Orion Research).

Open probability (P_o) was estimated by steady-state macroscopic recordings (when $P_o > 0.05$) and single-channel recordings in the same patch. nP_o was determined from all-points amplitude histograms by the sum of open levels (k) multiplied by fractional time spent (P_k): $nP_o = \Sigma kP_k$. To estimate the number of channels in a patch (n), maximum macroscopic conductance (G_{KMax}) was divided by single-channel conductance (g_k) at the same voltage for tail current measurements (−80 mV). $n = G_{KMax}/g_k$.

The steady-state data in 0 Ca²⁺ were fit to the Horrigan-Aldrich model (Horrigan and Aldrich, 2002) based on least-squares criteria. The following equations were used to estimate energetic changes associated with mutations (Ma et al., 2006):

$$\mathrm{C_0\text{-}O_0}: \Delta\Delta G = -kT\ln\frac{L_0^M}{L_0^{WT}};$$

$$\mathrm{C_4\text{-}C_0}: \Delta\Delta G = 4kT\ln\frac{J_0^M}{J_0^{WT}} \text{ and}$$

$$J_0 = \frac{0.5}{\exp\left(z_J Vh_c / kT\right)};$$

$$\mathrm{O_0\text{-}O_4}: \Delta\Delta G = -4kT\ln\frac{(J_0 D)^M}{(J_0 D)^{WT}} \text{ and}$$

$$J_0 D = \frac{0.5}{\exp\left(z_J Vh_o / kT\right)}; \text{ and}$$

$$\mathrm{O_4\text{-}C_4}: \Delta\Delta G = kT\ln\frac{L_0^M D^{M^4}}{L_0^{WT} D^{WT^4}}.$$

Online supplemental material
Fig. S1 shows that β1 and β4 share common gating effects. Fig. S2 shows effects of alanine substitutions of four β1 residues on G-V relations at various α/β1 molar ratios. Fig. S3 compares mutant P_o-V data in linear scale to best fits of the Horrigan-Aldrich model (see Table 2). Fig. S4 shows effects of I106A, Y74A, and Y105AY74A on free energies associated with various gating transitions. Online supplemental material is available at http://www.jgp.org/cgi/content/full/jgp.201110698/DC1.

RESULTS

Identifying β1 residues critical for gating modulation
Despite different physiological roles, both β1 and neuron-specific β4 subunits slow BK channel gating and modulate steady-state properties (Fig. S1, A and B). Compared with α alone channels, both β1 and β4 increase steady-state P_o at high Ca²⁺ but reduce it at low Ca²⁺ (Fig. S1 B). These steady-state effects are largely accounted for by two Ca²⁺-independent mechanisms. These are a reduction in intrinsic gating and a negative shift of open-channel voltage sensor activation (Fig. S1 C; Bao and Cox, 2005; Wang and Brenner, 2006; Wang et al., 2006; Sweet and Cox, 2009). Similarly, data from a previous study suggest that the dual gating mechanisms also underlie β2 modulation of BK channel properties (Orio and Latorre, 2005).

These prior findings led us to hypothesize that residues mediating gating modulation are conserved among
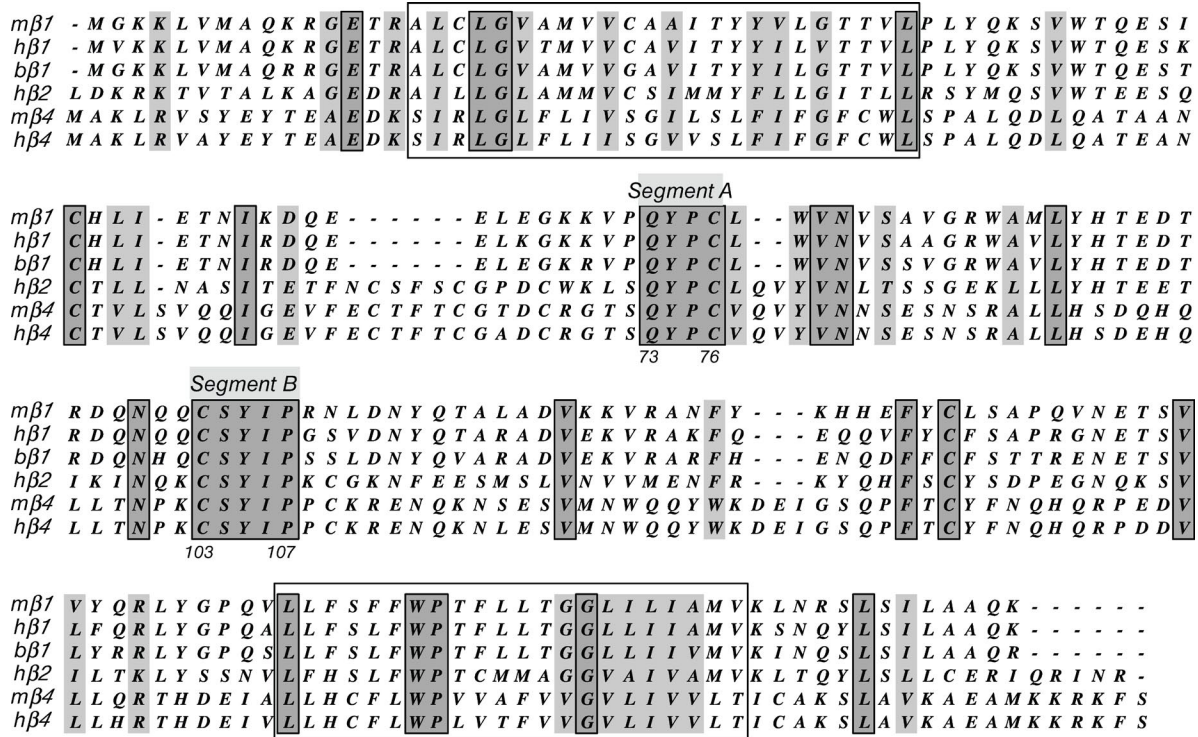
```
mβ1   - M G K K L V M A Q K R G E T R A L C L G V A M V V C A A I T Y Y V L G T T V L P L Y Q K S V W T Q E S I
hβ1   - M V K K L V M A Q K R G E T R A L C L G V T M V V C A V I T Y Y I L V T T V L P L Y Q K S V W T Q E S K
bβ1   - M G K K L V M A Q R R G E T R A L C L G V A M V V G A V I T Y Y I L G T T V L P L Y Q K S V W T Q E S T
hβ2   L D K R K T V T A L K A G E D R A I L L G L A M M V C S I M M Y F L L G I T L L R S Y M Q S V W T E E S Q
mβ4   M A K L R V S Y E Y T E A E D K S I R L G L F L I V S G I L S L F I F G F C W L S P A L Q D L Q A T A A N
hβ4   M A K L R V A Y E Y T E A E D K S I R L G L F L I I S G V V S L F I F G F C W L S P A L Q D L Q A T E A N

                                                            Segment A
mβ1   C H L I - E T N I K D Q E - - - - - - E L E G K K V P Q Y P C L - - W V N V S A V G R W A M L Y H T E D T
hβ1   C H L I - E T N I R D Q E - - - - - - E L K G K K V P Q Y P C L - - W V N V S A A G R W A V L Y H T E D T
bβ1   C H L I - E T N I R D Q E - - - - - - E L E G K R V P Q Y P C L - - W V N V S S V G R W A V L Y H T E D T
hβ2   C T L L - N A S I T E T F N C S F S C G P D C W K L S Q Y P C L Q V Y V N L T S S G E K L L L Y H T E E T
mβ4   C T V L S V Q Q I G E V F E C T F T C G T D C R G T S Q Y P C V Q V Y V N N S E S N S R A L L H S D Q H Q
hβ4   C T V L S V Q Q I G E V F E C T F T C G A D C R G T S Q Y P C V Q V Y V N N S E S N S R A L L H S D E H Q
                                                          73    76
      Segment B
mβ1   R D Q N Q Q C S Y I P R N L D N Y Q T A L A D V K K V R A N F Y - - - K H H E F Y C L S A P Q V N E T S V
hβ1   R D Q N Q Q C S Y I P G S V D N Y Q T A R A D V E K V R A K F Q - - - E Q Q V F Y C F S A P R G N E T S V
bβ1   R D Q N H Q C S Y I P S S L D N Y Q V A R A D V E K V R A R F H - - - E N Q D F F C F S T T R E N E T S V
hβ2   I K I N Q K C S Y I P K C G K N F E E S M S L V N V V M E N F R - - - K Y Q H F S C Y S D P E G N Q K S V
mβ4   L L T N P K C S Y I P P C K R E N Q K N S E S V M N W Q Q Y W K D E I G S Q P F T C Y F N Q H Q R P E D V
hβ4   L L T N P K C S Y I P P C K R E N Q K N L E S V M N W Q Q Y W K D E I G S Q P F T C Y F N Q H Q R P D D V
          103       107
mβ1   V Y Q R L Y G P Q V L L F S F F W P T F L L T G G L I L I A M V K L N R S L S I L A A Q K - - - - - -
hβ1   L F Q R L Y G P Q A L L F S L F W P T F L L T G G L L I I A M V K S N Q Y L S I L A A Q K - - - - - -
bβ1   L Y R R L Y G P Q S L L F S L F W P T F L L T G G L L I I V M V K I N Q S L S I L A A Q R - - - - - -
hβ2   I L T K L Y S S N V L F H S L F W P T C M M A G G V A I V A M V K L T Q Y L S L L C E R I Q R I N R -
mβ4   L L Q R T H D E I A L L H C F L W P V V A F V V G L V I V V L T I C A K S L A V K A E A M K K R K F S
hβ4   L L H R T H D E I V L L H C F L W P L V T F V V G L V I V V L T I C A K S L A V K A E A M K K R K F S
```

Figure 1. β1 residues conserved with family members β2 and β4. Sequence alignment of the β subunit family members, including mouse, human, and bovine β1, human β2, and mouse and human β4. The 28 identical residues are boxed and shaded in dark gray. The 28 conserved but nonidentical residues are shaded in light gray. The two TM regions, TM1 and TM2, and the two most conserved segments, A and B, are boxed.

β1, β2, and β4. To identify potential key gating residues and domains, we performed sequence alignment of mβ1, hβ1, bβ1, hβ2, mβ4, and hβ4 and identified two highly conserved segments (Fig. 1). Extracellular segment A consists of four identical residues ($Q_{73}YPC_{76}$), and segment B consists of five identical residues ($C_{103}SYIP_{107}$; Fig. 1). Segments A and B consist of the longest sequence of consecutive identical residues among these β subunits. To test the hypothesis that these conserved segments have important roles in gating modulation, we performed an alanine substitution mutagenesis of 13 identical residues within or neighboring segments A and B.

Mutant β1 ($β1_{MT}$) subunits were expressed at saturating concentrations with wild-type α subunits using transient transfection in HEK-293 cells. BK currents were recorded using the inside-out patch clamp configuration at 60 µM Ca^{2+} (Fig. 2 A). Averaged G-V relations of $αβ1_{MT}$ were compared with α alone and $αβ1_{WT}$ channels (Fig. 2, B and C). Mutations such as V120A caused a small or no change in channel properties (Fig. 2, B and C). In contrast, mutations such as S104A reduced the size of the G-V shift (by ∼30 mV; Fig. 2 B) and slowed the activation time constants (Fig. 2 C).

In addition to S104, we have identified three other positions that are important in mediating gating modulation. These include segment B residues Y105 and I106 as well as segment A residue Y74 (Fig. 3). Alanine substitu-

tions of these residues reduce β1-mediated G-V shifts, increasing $V_{1/2}$ by 28–44 mV (Fig. 3 A). These results are consistent with the hypothesis that segment A and B residues play an important role in gating modulation.

Segment A and B residues have nonadditive effects

Similar effects of alanine substitution of Y74, S104, Y105, and I106 suggest that these residues may contribute to common functional interactions. To test this hypothesis, we examined whether these mutations have additive effects. If the two residues contribute to a common interaction, effects of the double mutation should not exceed both single mutations.

We first examined segment B mutations Y105A and I106A (Fig. 4 A). Indeed, the steady-state effect of the double mutant Y105AI106A ($V_{1/2}$ of -48 ± 4 mV) is not significantly different from individual mutants Y105A (-45 ± 5 mV, $P \approx 0.6$) or I106A (-49 ± 5 mV, $P \approx 0.9$; Fig. 4 B, left). The nonadditive effects were also observed from activation kinetics. Compared with $β1_{WT}$, both single mutations slow activation, with I106A having a greater effect than Y105A. This kinetic effect of Y105AI106A is not significantly greater than I106A (Fig. 4 B, right). At -20 mV, time constants for I106A and Y105AI106A are 10.1 ± 1.5 ms and 14.2 ± 2.0 ms, respectively ($P \approx 0.1$). At -40 mV, they are 17.0 ± 1.3 ms and 21.4 ± 3.5 ms, respectively ($P \approx 0.3$).
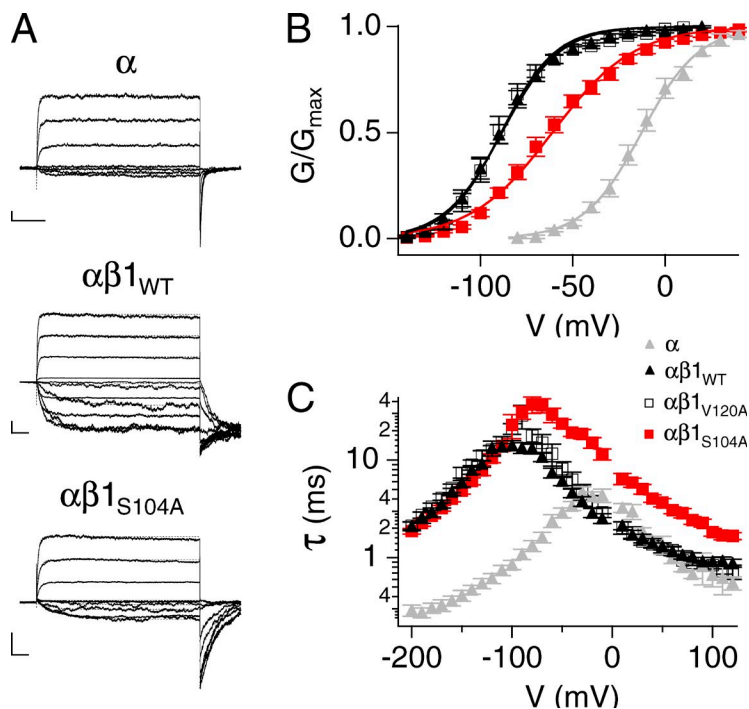
Figure 2. Alanine substitutions of key β1 residues affect the G-V relations and gating kinetics. (A) Families of currents recorded at 60 μM Ca^{2+} from BK channels composed of α subunit alone (α), α subunit coassembled wild-type β1 (αβ1$_{WT}$), or β1 with a single alanine substitution (αβ1$_{S104A}$). α currents were evoked by 100-ms depolarization in 20-mV steps between −60 and 60 mV. αβ1 currents were evoked by 200-ms depolarization in 20-mV steps between −140 and 60 mV. The x and y scale bars represent 20 ms and 0.5 nA, respectively. (B) Averaged G-V relations of αβ1$_{V120A}$ and αβ1$_{WT}$ largely overlap, indicating that the V120A mutation has little effect on steady-state modulation of the α subunit. In contrast, the S104A mutation shifts the G-V relations by ∼30 mV, reducing β1 steady-state modulatory effects. α, $n = 16$; αβ1$_{WT}$, $n = 12$; αβ1$_{S104A}$, $n = 32$; αβ1$_{V120A}$, $n = 11$. (C) S104A, but not V120A, alters β1 effects on activation kinetics. The averaged activation and deactivation time constants of α, αβ1$_{WT}$, αβ1$_{V120A}$, and αβ1$_{S104A}$ channels are shown, plotted as a function of voltage. α, $n = 9–16$; αβ1$_{WT}$, $n = 8–12$; αβ1$_{S104A}$, $n = 17–32$; αβ1$_{V120A}$, $n = 7–11$. Error bars represent SEM.

Next, we tested whether mutant effects of segment A and B residues Y74A and Y105A are additive (Fig. 4 C). The steady-state effect of Y105AY74A (V$_{1/2}$ of −48 ± 3 mV) is not significantly different from Y105A (−45 ± 5 mV, P ≈ 0.6) even though it is greater than Y74A (−57 ± 3 mV, P ≈ 0.03; Fig. 4 D, left). Similarly, kinetic effects

of the double mutation are not greater than those of Y105A (Fig. 4 D, right). At −20 mV, the activation time constant for Y105AY74A (7.2 ± 0.9 ms) is similar to Y105A (8.8 ± 1.0 ms, P ≈ 0.3) and Y74A (8.3 ± 0.7 ms, P ≈ 0.4). Finally, deactivation time constants are also not significantly different between Y105AY74A and

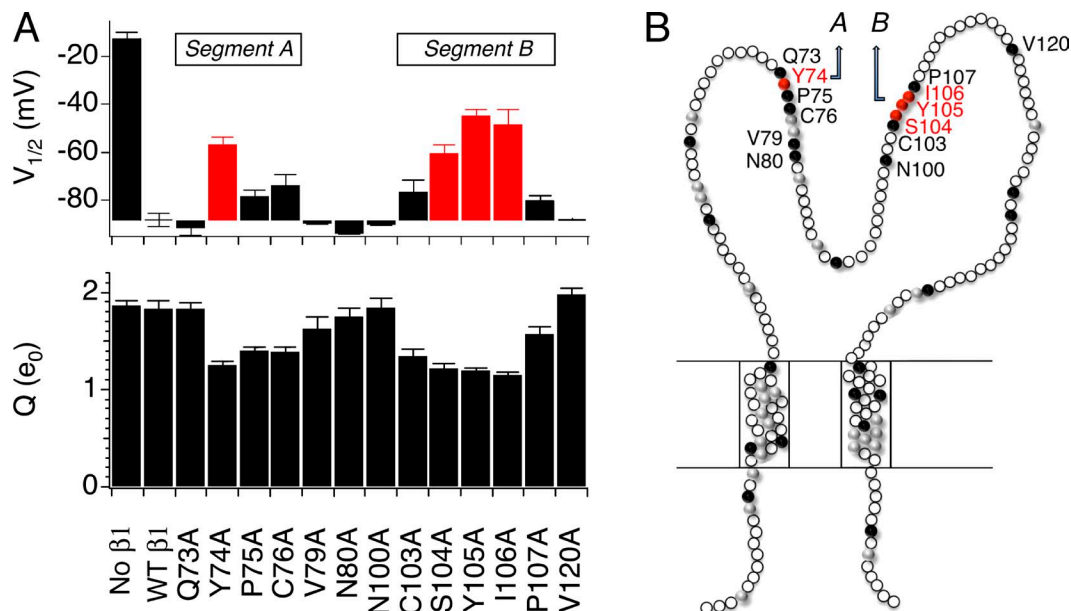**Figure 3.** Steady-state effects of mutations on β1 function. (A) Summarized steady-state effects of 13 alanine substitutions measured in 60 μM Ca^{2+}. Averaged V$_{1/2}$ (top) and Q (bottom) for BK channels with no β1, wild-type β1, or mutant β1. α, $n = 16$; αβ1$_{WT}$, $n = 12$; αβ1$_{Q73A}$, $n = 16$; αβ1$_{Y74A}$, $n = 15$; αβ1$_{P75A}$, $n = 16$; αβ1$_{C76A}$, $n = 20$; αβ1$_{V79A}$, $n = 14$; αβ1$_{N80A}$, $n = 6$; αβ1$_{N100A}$, $n = 6$; αβ1$_{C103A}$, $n = 8$; αβ1$_{S104A}$, $n = 32$; αβ1$_{Y105A}$, $n = 26$; αβ1$_{I106A}$, $n = 11$; αβ1$_{P107A}$, $n = 14$; αβ1$_{V120A}$, $n = 11$. Error bars represent SEM. (B) Positions of key segments A and B on a schematic cartoon of β1. Residues mutated to alanine are labeled with their respective amino acids. Mutated residues having relatively large and small effects are represented by closed red and black circles, respectively. Identical and nonidentical but conserved residues in other positions are represented by closed black and gray circles, respectively.
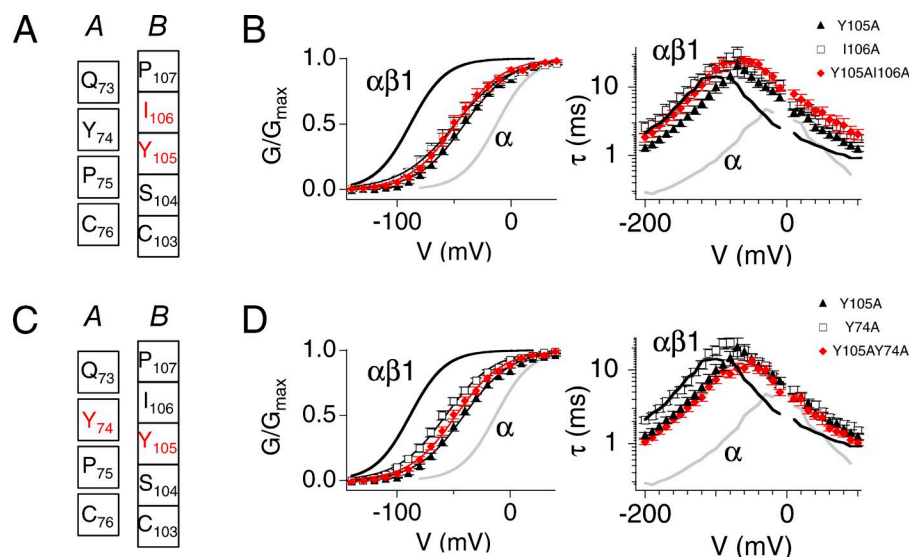
Figure 4. Alanine substitution of segment A and B residues displays nonadditive effects. (A) Both Y105 and I106 resides in segment B. (B) The effects of Y105A and I106A are nonadditive. (left) The positive shift of G-V by Y105AI106A ($n = 10$) is not greater than Y105A ($n = 26$) or I106A ($n = 11$). (right) Y105AI106A ($n = 8$–10) does not slow activation time constants more than both single mutations. $\alpha\beta1_{Y105A}$, $n = 13$–24; $\alpha\beta1_{I106A}$, $n = 8$–11. (C) Y105 and Y74 reside in segment B and A, respectively. (D) The effects of Y105A and Y74A are nonadditive. (left) The positive shift of G-V by Y105AY74A ($n = 24$) is not greater than Y105A. (right) Y105AY74A ($n = 22$–24) does not slow activation or speed deactivation time constants more than either single mutation. $\alpha\beta1_{Y74A}$, $n = 8$–14; $\alpha\beta1_{Y105A}$, $n = 13$–24. (B and D, left) The black and gray traces represent Boltzmann fits of averaged G-V relations of $\alpha\beta1$ and α channels, respectively. (right) The black and gray traces represent averaged activation and deactivation time constants of $\alpha\beta1$ and α channels, respectively. Error bars represent SEM.

Y105A. For example, at -200 mV, deactivation time constants are 1.3 ± 0.2 ms and 1.1 ± 0.1 ms, respectively ($P \approx 0.1$).

The aforementioned results show that at 60 µM Ca^{2+}, steady-state and kinetic effects of segment A and B mutations are nonadditive, suggesting that these residues functionally interact in modulating BK channel gating. The BK channel dual allosteric gating model includes a gate, four independent voltage sensors, and four Ca^{2+} sensors (Rothberg and Magleby, 2000; Horrigan and
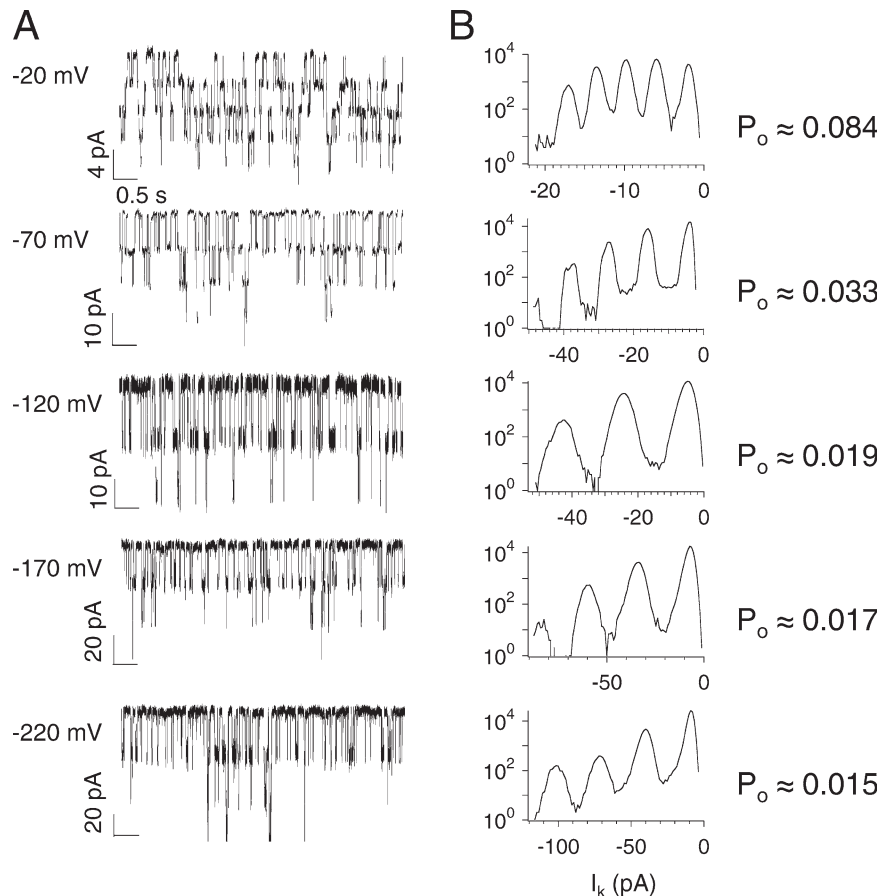

Figure 5. Measurement of P_o at 0 Ca^{2+} and the limiting slope using F380Y. (A) Representative single-channel recordings of α_{F380Y} channels at 0 Ca^{2+} and decreasing voltages. (B) Corresponding all-point amplitude histograms and estimates of P_o. The estimated number of channels in the patch is 74.
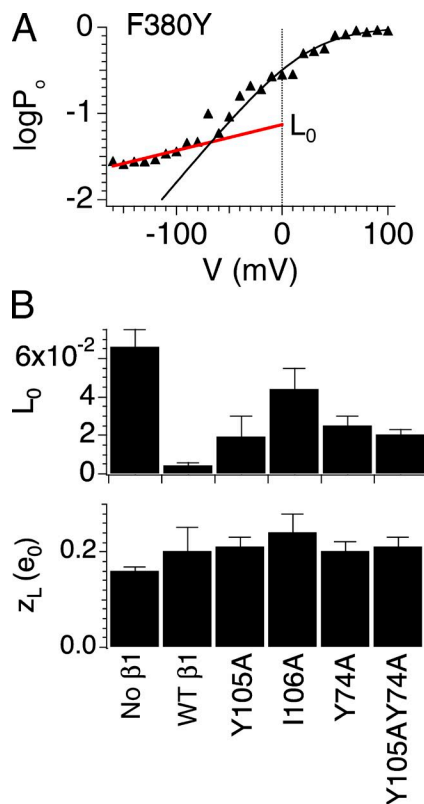
Figure 6. Segment A and B residues contribute to reducing intrinsic opening. (A) A representative $logP_o$-V relation of α_{F380Y} channel in which the limiting slope was fitted to the Horrigan-Aldrich model to estimate z_L and L_0. The black curve represents the Boltzmann fit plotted in a log scale (right axis not shown, axis range 0.01–1). The red line represents the linear fits of $logP_o$-V relations to the Horrigan-Aldrich model between -160 and -90 mV. Weak voltage dependence of P_o at the limiting slope is apparent when compared with the Boltzmann fit. (B) Averaged estimates for L_0 and z_L for different channel configurations. No β1, $n = 5$; WT β1, $n = 7$; Y105A, $n = 8$; I106A, $n = 8$; Y74A, $n = 9$; Y105AY74A, $n = 9$. Error bars represent SEM.

Aldrich, 2002). Channel opening is allosterically coupled to voltage sensor activation and Ca^{2+} binding. However, channels can open at a low probability independent of voltage sensor activation and Ca^{2+} binding (intrinsic gating). Previously, β1 subunits have been shown to confer modulatory effects on intrinsic gating, voltage sensor activation, and Ca^{2+} binding (Cox and Aldrich, 2000; Nimigean and Magleby, 2000; Bao and Cox, 2005; Orio and Latorre, 2005; Wang and Brenner, 2006; Sweet and Cox, 2009). Because segments A and B are located in the extracellular region, we focused on how these domains modulate Ca^{2+}-independent effects: intrinsic gating and voltage sensor activation.

Segment A and B residues reduce intrinsic gating
Intrinsic gating is weakly voltage dependent and can be described by two free parameters (Horrigan and Aldrich, 2002). L_0 represents the zero voltage value of the closed-

to-open (C-O) equilibrium constant, and z_L is its partial charge (Horrigan and Aldrich, 2002). To isolate mutant effects on intrinsic gating, we performed recordings using a modified α subunit F380Y. Previously, this modification has been shown to greatly increase channel opening in hslo1 (Lippiat et al., 2000) and mslo1 (Wang and Brenner, 2006). F380Y allows us to measure channel P_o in ligand-unbound states (0 Ca^{2+}) with voltage sensors residing in the resting state (the limiting slope). In α_{WT} background, obtaining P_o under these conditions is not technically feasible for the αβ1 channels ($P_o < 10^{-8}$; Wang and Brenner, 2006).

An example recording of α subunit F380Y in 0 Ca^{2+} over a range of voltages is shown in Fig. 5 A. The corresponding all-point histograms and estimated P_o (Fig. 5 B) clearly show that the voltage dependence approaches a minimum between -120 and -220 mV. The estimated weak voltage dependence here ($\sim$0.25 e_0) corresponds to the weak voltage dependence associated with intrinsic gating (z_L; Horrigan and Aldrich, 2002). Fitting 0 Ca^{2+} limiting slope $logP_o$-V relations to the Horrigan-Aldrich model (Horrigan and Aldrich, 2002), the two free parameters associated with intrinsic gating were estimated (L_0 of 6.6 ± 0.9 e^{-2} and z_L of 0.16 ± 0.01 e_0; Fig. 6 A and Table 1). For α_{F380Y}, the effect of $β1_{WT}$ on intrinsic gating is an $\sim$15-fold reduction in L_0 (4.3 ± 1.9 e^{-3}, P < 0.001). However, z_L is not significantly altered (0.20 ± 0.05 e_0, P ≈ 0.5; Table 1).

L_0 is significantly increased by segment A and B key mutations (Table 1). In the presence of Y105A, I106A, or Y74A, L_0 are 1.9 ± 0.4, 4.4 ± 1.1, or 2.5 ± 0.5 e^{-2} (Table 1). The $\sim$4-, 10-, and 6-fold increases of L_0 (relative to $\alpha_{F380Y}β1_{WT}$ channels) reflect a reduction in β1's ability to decrease intrinsic gating. The results suggest an important role that Y105, I106, and Y74 play in β1 modulation of intrinsic gating.

Double mutation Y105AY74A was also examined to test whether effects of Y105A and Y74A on intrinsic gating were additive. If effects of Y105A and Y74A on intrinsic gating were additive, a significant increase in L_0 would have been expected. Because the estimated L_0 for $\alpha_{F380Y}β1_{Y105AY74A}$, 2.0 ± 0.3 e^{-2}, is similar to the single mutations, the results suggest that segments A and B functionally interact in reducing intrinsic gating.

Segment A and B residues modulate open-channel voltage sensor activation
An increase in L_0 predicts an increase in steady-state opening at all Ca^{2+}. This is unlikely to be the sole effect of segment A and B mutants because the mutations displayed positive shifts of G-V relations. We therefore investigated whether these mutations also alter voltage sensor activation. Voltage sensor activation of unliganded channels is described by three free parameters: the partial charge associated with the resting-to-activated (R-A) transition (z_J) and the half-activation voltages for voltage

TABLE 1
Steady-state intrinsic gating parameters

Channels α_{F380Y}	L_0	P-value	z_L	P-value (approximately)	$\Delta\Delta G$	n
	e^{-2}		e_0		$kcal/mol$	
No β1	6.6 ± 0.9	<0.001	0.16 ± 0.01	0.5		5
WT β1	4.3 ± 1.9[a]	NA	0.20 ± 0.05	NA	1.62	7
β1$_{Y105A}$	1.9 ± 0.4	<0.01	0.21 ± 0.02	0.8	0.74	8
β1$_{I106A}$	4.4 ± 1.1	<0.01	0.24 ± 0.04	0.5	0.39	8
β1$_{Y74A}$	2.5 ± 0.5	<0.01	0.20 ± 0.02	0.7	0.58	9
β1$_{Y74AY105A}$	2.0 ± 0.3	<0.001	0.21 ± 0.02	0.9	0.71	9

NA, not applicable.

[a]e^{-3}.

sensors of open and closed channels (Vh_o and Vh_c, respectively; Horrigan and Aldrich, 2002). The R-A equilibrium constant of closed, unliganded channel J_0 (the zero voltage value of the R-A equilibrium constant) is a function of Vh_c ($J_0 = 0.5/\exp(z_J Vh_c/kT)$). The allosteric factor between the voltage sensor activation and gating (D) is a function of the difference between Vh_c and Vh_o ($D = 0.5/\exp(z_J(Vh_c - Vh_o)/kT)$; Horrigan and Aldrich, 2002).

We obtained 0 Ca^{2+} P_o over a wide range of voltages. Averaged $logP_o$-V and P_o-V relations data were fit to the Horrigan-Aldrich model (Fig. 7 and Fig. S3; Horrigan and Aldrich, 2002). In all these fits, z_L and z_J were set as 0.2 e_0 and 0.58 e_0, respectively, to reduce the number of free parameters. The basis for our assumptions here are twofold. First, the finding that voltage sensors act as a source of gating charge for the opening transition (Ma et al., 2006) and the observation that the mutations do not alter z_L imply that these mutations do not significantly alter z_J as well. Second, prior gating current data

found that neither z_L nor z_J are altered by β1 (Bao and Cox, 2005), suggesting that mutations likely do not alter z_L or z_J either.

The fits to the $logP_o$-V relations (Table 2) show that β1 stabilizes voltage sensor activation in both open and closed channels. There is a −55-mV shift of the half-activating voltage for the open-channel voltage sensor (Vh_o), similar to the −61-mV value estimated in the α_{WT} background (Bao and Cox, 2005). α_{F380Y} reports a −37-mV shift of the half-activating voltage for the closed-channel voltage sensor (Vh_c), which is smaller than the −71-mV value estimated in the α_{WT} background (Bao and Cox, 2005).

Y105A has little effect on closed-channel voltage sensor activation. This is evident from estimates of Vh_c (76 vs. 73 mV) and the corresponding R-A equilibrium J_0 (8.8 vs. 9.4 e^{-2}; Table 2). However, the mutation destabilizes open-channel voltage sensor activation (13 vs. −10 mV), thereby reducing the allosteric coupling between voltage sensor activation and gating (D of 3.9 vs. 7.1; Table 2).
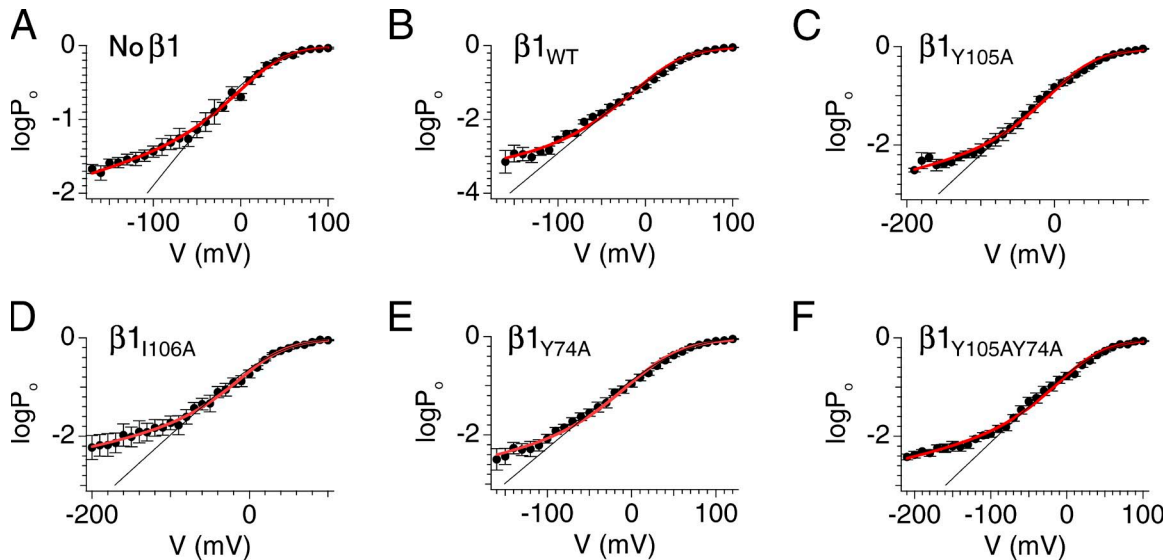

Figure 7. Segment A and B residues contribute to stabilization of open-channel voltage sensor activation. (A–F) Averaged $logP_o$-V relations (circles) and best fits to the Horrigan-Aldrich model (red curves). The black curves represent Boltzmann fits. No β1, $n = 5–13$; WT β1, $n = 3–30$; Y105A, $n = 7–24$; I106A, $n = 4–8$; Y74A, $n = 5–12$; Y105AY74A, $n = 6–12$. Error bars represent SEM.

Channels	Intrinsic gating (L_0)	Voltage sensor activation			
		Vh_o	Vh_c	J_0	D
	e^{-2}	mV	mV	e^{-2}	
α_{F380Y}	6.9	45	113	3.8	4.7
$\alpha_{F380Y}\beta1_{WT}$	2.5[a]	−10	76	8.8	7.1
$\alpha_{F380Y}\beta1_{Y105A}$	1.4	13	73	9.4	3.9
$\alpha_{F380Y}\beta1_{I106A}$	2.9	19	80	8.0	4.0
$\alpha_{F380Y}\beta1_{Y74A}$	1.3	14	75	9.0	4.0
$\alpha_{F380Y}\beta1_{Y74AY105A}$	1.8	11	72	9.7	4.0

[a]e^{-3}.

Similarly, mutating I106 and Y74 also destabilize open-channel voltage sensor activation, increasing Vh_o by 29 mV and 24 mV, respectively (Table 2). Finally, Y105AY74A increases Vh_o by 21 mV (Table 2), suggesting that effects
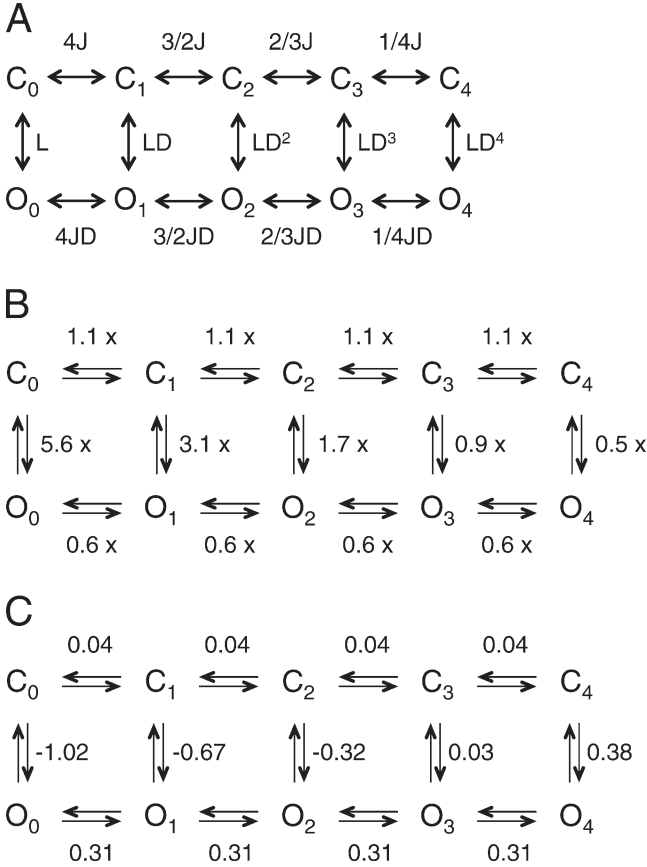

Figure 8. Effects of Y105A on intrinsic gating and voltage sensor activation. (A) The 10-state gating scheme for unliganded BK channel in the Horrigan-Aldrich model (Horrigan and Aldrich, 2002). C and O represent closed and open channels, respectively. Subscripts represent the number of activated voltage sensors per channel. Equilibrium constants are indicated. (B) Numbers indicate effects of the Y105A mutation on equilibrium constants. (C) Numbers indicate effects of the Y105A mutation on free energies.

of single mutations are nonadditive. Therefore, segments A and B may functionally interact in stabilizing voltage sensor activation in open channels.

Effects of the segment A-B domain on gating energetics

The aforementioned results indicate that the segment A-B domain mediates two gating effects: reduction of intrinsic gating and stabilization of voltage sensor activation in open channels. The fact that a single functional domain underlies both gating effects suggests obligatory coupling of the two. We have calculated mutant effects on the free energy changes associated with the C-O and R-A transitions to more closely examine how the segment A-B domain exerts the dual gating effects.

Fig. 8 A plots the 10-state gating scheme for unliganded channels. Channels reside in either closed (C) or open (O) states with zero to four activated voltage sensors (Horrigan and Aldrich, 2002). The effects of segment A-B mutations on the steady-state equilibrium constant and free energy associated with each transition were plotted in Fig. 8 (B and C, respectively). The Y105A mutation has little effect (1.1-fold, 0.04 kcal/mol) on the R-A equilibrium of closed channels (Fig. 8, B and C). However, the mutation increases the energetic barrier (0.6-fold, 0.31 kcal/mol) of the R-A transitions of open states (Fig. 8, B and C). The largest effects are increases of the early C-O transitions in which no or few voltage sensors are active (i.e., 5.6-fold, −1.02 kcal/mol for C_0-O_0; Fig. 8, B and C). These effects are quantitatively similar in mutations I106A, Y74A, and Y74AY105A (Fig. S3 and summarized in Table 3). From the perspective of the wild-type β subunit, a simple model that explains these results is one in which segment A-B interactions cause a destabilization of early open states (O_0 to O_2) but have little effect on closed states.

DISCUSSION

Our scan identified four residues critical for β1 gating modulation. Mutating these residues reduce β1-mediated negative G-V shift at 60 Ca^{2+}, consistent with a partial disruption in β1 function. The experimental evidence does not suggest gain-of-function mutant effects. For example, gating parameters normally not altered by $β1_{WT}$ (such as z_L) are also not altered by these mutations, and gating parameters normally altered by $β1_{WT}$ (such as L_0 and Vh_o) are reduced by these mutations.

Previous studies suggest that β1 alters several gating parameters of BK channels (Cox and Aldrich, 2000; Bao and Cox, 2005; Orio and Latorre, 2005; Orio et al., 2006; Wang and Brenner, 2006; Sweet and Cox, 2009). Our observations that no single mutation eliminated β1-mediated negative G-V shift or free energy changes suggest that additional key gating residues remain to be uncovered. This is true even for the effects on intrinsic gating and open-channel voltage sensor activation that

TABLE 3

Free energy change relative to wild-type β1

Channels	$\Delta\Delta G$			
α_{F380Y}				
	C_0-O_0	O_0-O_4	O_4-C_4	C_4-C_0
	kcal/mol			
No β1	−1.96	2.96	0.99	−1.99
β1$_{Y105A}$	−1.02	1.24	−0.38	0.16
β1$_{I106A}$	−1.45	1.56	0.10	−0.22
β1$_{Y74A}$	−0.97	1.29	−0.37	0.05
β1$_{Y74AY105A}$	−1.16	1.13	−0.18	0.22

mutants did not completely eliminate. Most likely, multiple independent interactions mediate β1 gating effects. These include Ca^{2+}-dependent effects that are difficult to gauge using α_{F380Y} and therefore are not addressed in this study.

Our finding that mutations of β1 disrupt effects on intrinsic gating and voltage sensor activation is consistent with previous studies ascribing β1 modulation of BK channels to these two effects (Nimigean and Magleby, 2000; Bao and Cox, 2005; Orio and Latorre, 2005; Wang and Brenner, 2006). Indeed, mutations of the BK channel voltage sensor have been suggested to specifically occlude the β1-mediated negative G-V shift (Yang et al., 2008). Based on the observation that single-residue mutations both reduce the energetic barrier for intrinsic opening and increase the energetic barrier for open-channel voltage sensor activation, a novel insight provided by the current study is that β1 modulation of these two aspects of gating is likely coupled. Because previous studies have identified single α mutations that alter both

intrinsic opening and voltage sensor activation (Ma et al., 2006; Wang and Brenner, 2006), this coupling may reflect intrinsic properties of the pore-forming subunit rather than properties unique to β1 function.

The dual gating effects of the segment A-B domain likely contribute to the complex steady-state modulatory effects of β subunits (Fig. S1). Interactions involving the segment A-B domain transition the channel away from open states with relaxed voltage sensors (the OR state; Fig. 9). Thus, in the absence of calcium or membrane depolarization, β1 causes a relative destabilization of the OR state and "silences" the channel in the closed resting state (CR; Fig. 9). With sufficient depolarization and/or calcium, β1 promotes channel opening by facilitating transitions to the late opening states (the OA state; Fig. 9).

Our results suggest that the segment A-B domain is necessary for maintaining the regulatory effects of β1. The data do not exclude the possibility that this domain plays an indirect role, simply being required to maintain a particular β or α/β subunit structure necessary for β1 subunit gating effects. However, the fact that segments A and B are the most conserved domain led us to favor a simpler scenario that this domain mediates the modulatory effects directly.

Several studies suggest that the extracellular segments A and B may be positioned near the external vestibule of BK channels (Fig. 9). Extracellular residues of β subunits have been shown to affect charybdotoxin binding and instantaneous I-V relations (Hanner et al., 1998; Zeng et al., 2003; Chen et al., 2008). Interestingly, hβ2 lysine residues flanking segment B (Fig. 1) have been shown to confer outward rectification of BK currents

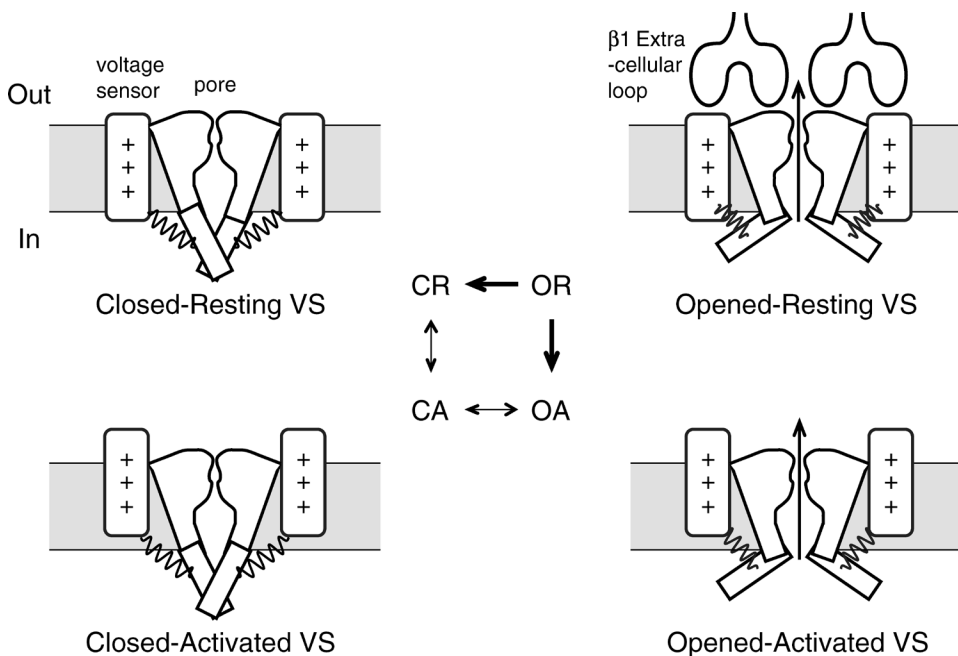**Figure 9.** A hypothetical mechanism for β1 function. Cartoons illustrate how the β1 extracellular domain may affect both intrinsic gating and voltage sensor (VS) activation. The pore and voltage sensor domains are depicted in four combinations: closed resting (CR), open resting (OR), open activated (OA), and closed activated (CA). The segment A-B domain promotes transitions away from open states with no or few voltage sensors activated (OR). At rest, the domain reduces opening by causing a relative destabilization of the OR state and promoting transitions to the CR states. With sufficient depolarization, the domain stabilizes channel opening by promoting transitions to the late opening states (OA). The segment A-B domain may selectively interact with the open but not closed channels.

(Chen et al., 2008). These results suggest close approximation between the outer vestibule of the channel and the β subunit extracellular domain (including the segment B region). Assuming the role of the segment A-B domain is direct, how do β subunit residues near the external mouth of BK channels modulate gating? There has been compelling evidence that suggests the selectivity filter is the activation gate for BK channels (Li and Aldrich, 2004; Piskorowski and Aldrich, 2006; Wilkens and Aldrich, 2006; Chen and Aldrich, 2011; Cox and Hoshi, 2011; Geng et al., 2011; Zhou et al., 2011). Proximity between the outer vestibule and the selectivity filter suggests that the segment A-B domain may be positioned near the gate. Our finding that the segment A and B mutations affect both voltage sensing and intrinsic gating presents the intriguing possibility that this domain may interact at a nexus for coupling open-channel voltage sensor to the selectivity filter/channel gate. Indeed, it will be interesting to determine whether physical interactions between the segment A-B domain and the pore-forming subunits are state dependent (i.e., interactions only occurring in open states; Fig. 9).

Alternatively, the segment A-B domain may interact with the pore-forming subunits indirectly, via other extracellular residues or other parts of the channel. Using chimera and deletion approaches, the intracellular domains of β1 have also been shown to be important for β1 function (Orio et al., 2006; Wang and Brenner, 2006). In addition, β1 TMs have been shown to lay interposed between voltage sensor domains of adjacent α subunits (Liu et al., 2010), suggesting a role these domains play in modulating voltage sensor activation. The relations among various β subunit domains and their relevant contributions remain an important question to be addressed in future studies.

In summary, this study identifies an important domain of β1 subunits that underlies, in part, modulation of BK/β1 channels. The reduced intrinsic opening conferred by the segment A-B domain and increased voltage sensor activation created a steeper activation response of BK channels associated with β1. The fact that human β1 polymorphisms with more moderate gating effects have been linked to decreased prevalence of hypertension and reduced pulmonary function (Fernández-Fernández et al., 2004; Seibold et al., 2008) highlights the potential physiological importance of the segment A-B domain in β1 and perhaps other β subunits.

REFERENCES

Atkinson, N.S., G.A. Robertson, and B. Ganetzky. 1991. A component of calcium-activated potassium channels encoded by the *Drosophila* slo locus. *Science*. 253:551–555. http://dx.doi.org/10.1126/science.1857984

Bao, L., and D.H. Cox. 2005. Gating and ionic currents reveal how the BK_{Ca} channel's Ca^{2+} sensitivity is enhanced by its β1 subunit. *J. Gen. Physiol.* 126:393–412. http://dx.doi.org/10.1085/jgp.200509346

Behrens, R., A. Nolting, F. Reimann, M. Schwarz, R. Waldschütz, and O. Pongs. 2000. hKCNMB3 and hKCNMB4, cloning and characterization of two members of the large-conductance calcium-activated potassium channel beta subunit family. *FEBS Lett.* 474:99–106. http://dx.doi.org/10.1016/S0014-5793(00)01584-2

Brenner, R., T.J. Jegla, A. Wickenden, Y. Liu, and R.W. Aldrich. 2000a. Cloning and functional characterization of novel large conductance calcium-activated potassium channel beta subunits, hKCNMB3 and hKCNMB4. *J. Biol. Chem.* 275:6453–6461. http://dx.doi.org/10.1074/jbc.275.9.6453

Brenner, R., G.J. Peréz, A.D. Bonev, D.M. Eckman, J.C. Kosek, S.W. Wiler, A.J. Patterson, M.T. Nelson, and R.W. Aldrich. 2000b. Vasoregulation by the beta1 subunit of the calcium-activated potassium channel. *Nature*. 407:870–876. http://dx.doi.org/10.1038/35038011

Calderone, V. 2002. Large-conductance, ca(2+)-activated k(+) channels: function, pharmacology and drugs. *Curr. Med. Chem.* 9:1385–1395.

Chen, M., G. Gan, Y. Wu, L. Wang, Y. Wu, and J. Ding. 2008. Lysine-rich extracellular rings formed by hbeta2 subunits confer the outward rectification of BK channels. *PLoS ONE*. 3:e2114. http://dx.doi.org/10.1371/journal.pone.0002114

Chen, X., and R.W. Aldrich. 2011. Charge substitution for a deep-pore residue reveals structural dynamics during BK channel gating. *J. Gen. Physiol.* 138:137–154. http://dx.doi.org/10.1085/jgp.201110632

Cox, D.H., and R.W. Aldrich. 2000. Role of the β1 subunit in large-conductance Ca^{2+}-activated K^+ channel gating energetics. Mechanisms of enhanced Ca^{2+} sensitivity. *J. Gen. Physiol.* 116:411–432. http://dx.doi.org/10.1085/jgp.116.3.411

Cox, D.H., and T. Hoshi. 2011. Where's the gate? Gating in the deep pore of the BK_{Ca} channel. *J. Gen. Physiol.* 138:133–136. http://dx.doi.org/10.1085/jgp.201110681

Fernández-Fernández, J.M., M. Tomás, E. Vázquez, P. Orio, R. Latorre, M. Sentí, J. Marrugat, and M.A. Valverde. 2004. Gain-of-function mutation in the KCNMB1 potassium channel subunit is associated with low prevalence of diastolic hypertension. *J. Clin. Invest.* 113:1032–1039.

Geng, Y., X. Niu, and K.L. Magleby. 2011. Low resistance, large dimension entrance to the inner cavity of BK channels determined by changing side-chain volume. *J. Gen. Physiol.* 137:533–548. http://dx.doi.org/10.1085/jgp.201110616

Gribkoff, V.K., J.E. Starrett Jr., and S.I. Dworetzky. 1997. The pharmacology and molecular biology of large-conductance calcium-activated (BK) potassium channels. *Adv. Pharmacol.* 37:319–348. http://dx.doi.org/10.1016/S1054-3589(08)60954-0

Hanner, M., R. Vianna-Jorge, A. Kamassah, W.A. Schmalhofer, H.G. Knaus, G.J. Kaczorowski, and M.L. Garcia. 1998. The beta subunit of the high conductance calcium-activated potassium channel. Identification of residues involved in charybdotoxin binding. *J. Biol. Chem.* 273:16289–16296. http://dx.doi.org/10.1074/jbc.273.26.16289

Horrigan, F.T., and R.W. Aldrich. 2002. Coupling between voltage sensor activation, Ca^{2+} binding and channel opening in large conductance (BK) potassium channels. *J. Gen. Physiol.* 120:267–305. http://dx.doi.org/10.1085/jgp.20028605

Kaczorowski, G.J., H.G. Knaus, R.J. Leonard, O.B. McManus, and M.L. Garcia. 1996. High-conductance calcium-activated potassium channels; structure, pharmacology, and function.

J. Bioenerg. Biomembr. 28:255–267. http://dx.doi.org/10.1007/BF02110699

Knaus, H.G., K. Folander, M. Garcia-Calvo, M.L. Garcia, G.J. Kaczorowski, M. Smith, and R. Swanson. 1994. Primary sequence and immunological characterization of beta-subunit of high conductance Ca(2+)-activated K+ channel from smooth muscle. *J. Biol. Chem.* 269:17274–17278.

Lee, U.S., and J. Cui. 2010. BK channel activation: structural and functional insights. *Trends Neurosci.* 33:415–423. http://dx.doi.org/10.1016/j.tins.2010.06.004

Li, W., and R.W. Aldrich. 2004. Unique inner pore properties of BK channels revealed by quaternary ammonium block. *J. Gen. Physiol.* 124:43–57. http://dx.doi.org/10.1085/jgp.200409067

Lippiat, J.D., N.B. Standen, and N.W. Davies. 2000. A residue in the intracellular vestibule of the pore is critical for gating and permeation in Ca2+-activated K+ (BKCa) channels. *J. Physiol.* 529:131–138. http://dx.doi.org/10.1111/j.1469-7793.2000.00131.x

Lippiat, J.D., N.B. Standen, I.D. Harrow, S.C. Phillips, and N.W. Davies. 2003. Properties of BK(Ca) channels formed by bicistronic expression of hSloalpha and beta1-4 subunits in HEK293 cells. *J. Membr. Biol.* 192:141–148. http://dx.doi.org/10.1007/s00232-002-1070-0

Liu, G., X. Niu, R.S. Wu, N. Chudasama, Y. Yao, X. Jin, R. Weinberg, S.I. Zakharov, H. Motoike, S.O. Marx, and A. Karlin. 2010. Location of modulatory β subunits in BK potassium channels. *J. Gen. Physiol.* 135:449–459. http://dx.doi.org/10.1085/jgp.201010417

Ma, Z., X.J. Lou, and F.T. Horrigan. 2006. Role of charged residues in the S1-S4 voltage sensor of BK channels. *J. Gen. Physiol.* 127:309–328. http://dx.doi.org/10.1085/jgp.200509421

Nimigean, C.M., and K.L. Magleby. 2000. Functional coupling of the β_1 subunit to the large conductance Ca^{2+}-activated K+ channel in the absence of Ca^{2+}. Increased Ca^{2+} sensitivity from a Ca^{2+}-independent mechanism. *J. Gen. Physiol.* 115:719–736. http://dx.doi.org/10.1085/jgp.115.6.719

Orio, P., and R. Latorre. 2005. Differential effects of β1 and β2 subunits on BK channel activity. *J. Gen. Physiol.* 125:395–411. http://dx.doi.org/10.1085/jgp.200409236

Orio, P., P. Rojas, G. Ferreira, and R. Latorre. 2002. New disguises for an old channel: MaxiK channel beta-subunits. *News Physiol. Sci.* 17:156–161.

Orio, P., Y. Torres, P. Rojas, I. Carvacho, M.L. Garcia, L. Toro, M.A. Valverde, and R. Latorre. 2006. Structural determinants for functional coupling between the β and α subunits in the Ca^{2+}-activated K+ (BK) channel. *J. Gen. Physiol.* 127:191–204. http://dx.doi.org/10.1085/jgp.200509370

Piskorowski, R.A., and R.W. Aldrich. 2006. Relationship between pore occupancy and gating in BK potassium channels. *J. Gen. Physiol.* 127:557–576. http://dx.doi.org/10.1085/jgp.200509482

Plüger, S., J. Faulhaber, M. Fürstenau, M. Löhn, R. Waldschütz, M. Gollasch, H. Haller, F.C. Luft, H. Ehmke, and O. Pongs. 2000. Mice with disrupted BK channel beta1 subunit gene feature abnormal Ca(2+) spark/STOC coupling and elevated blood pressure. *Circ. Res.* 87:E53–E60.

Riazi, M.A., P. Brinkman-Mills, A. Johnson, S.L. Naylor, S. Minoshima, N. Shimizu, A. Baldini, and H.E. McDermid. 1999. Identification of a putative regulatory subunit of a calcium-activated potassium channel in the dup(3q) syndrome region and a related sequence on 22q11.2. *Genomics.* 62:90–94. http://dx.doi.org/10.1006/geno.1999.5975

Rothberg, B.S., and K.L. Magleby. 2000. Voltage and Ca^{2+} activation of single large-conductance Ca^{2+}-activated K+ channels described by a two-tiered allosteric gating mechanism. *J. Gen. Physiol.* 116:75–99.

Seibold, M.A., B. Wang, C. Eng, G. Kumar, K.B. Beckman, S. Sen, S. Choudhry, K. Meade, M. Lenoir, H.G. Watson, et al. 2008. An african-specific functional polymorphism in KCNMB1 shows sex-specific association with asthma severity. *Hum. Mol. Genet.* 17:2681–2690. http://dx.doi.org/10.1093/hmg/ddn168

Sweet, T.B., and D.H. Cox. 2009. Measuring the influence of the BK_{Ca} β1 subunit on Ca^{2+} binding to the BK_{Ca} channel. *J. Gen. Physiol.* 133:139–150. http://dx.doi.org/10.1085/jgp.200810129

Tanaka, Y., P. Meera, M. Song, H.G. Knaus, and L. Toro. 1997. Molecular constituents of maxi KCa channels in human coronary smooth muscle: predominant alpha + beta subunit complexes. *J. Physiol.* 502:545–557. http://dx.doi.org/10.1111/j.1469-7793.1997.545bj.x

Wallner, M., P. Meera, and L. Toro. 1999. Molecular basis of fast inactivation in voltage and Ca2+-activated K+ channels: a transmembrane beta-subunit homolog. *Proc. Natl. Acad. Sci. USA.* 96:4137–4142. http://dx.doi.org/10.1073/pnas.96.7.4137

Wang, B., and R. Brenner. 2006. An S6 mutation in BK channels reveals β1 subunit effects on intrinsic and voltage-dependent gating. *J. Gen. Physiol.* 128:731–744. http://dx.doi.org/10.1085/jgp.200609596

Wang, B., B.S. Rothberg, and R. Brenner. 2006. Mechanism of β4 subunit modulation of BK channels. *J. Gen. Physiol.* 127:449–465. http://dx.doi.org/10.1085/jgp.200509436

Wilkens, C.M., and R.W. Aldrich. 2006. State-independent block of BK channels by an intracellular quaternary ammonium. *J. Gen. Physiol.* 128:347–364. http://dx.doi.org/10.1085/jgp.200609579

Xia, X.M., J.P. Ding, and C.J. Lingle. 1999. Molecular basis for the inactivation of Ca2+- and voltage-dependent BK channels in adrenal chromaffin cells and rat insulinoma tumor cells. *J. Neurosci.* 19:5255–5264.

Yan, J., and R.W. Aldrich. 2010. LRRC26 auxiliary protein allows BK channel activation at resting voltage without calcium. *Nature.* 466:513–516. http://dx.doi.org/10.1038/nature09162

Yang, H., G. Zhang, J. Shi, U.S. Lee, K. Delaloye, and J. Cui. 2008. Subunit-specific effect of the voltage sensor domain on Ca2+ sensitivity of BK channels. *Biophys. J.* 94:4678–4687. http://dx.doi.org/10.1529/biophysj.107.121590

Zeng, X.H., X.M. Xia, and C.J. Lingle. 2003. Redox-sensitive extracellular gates formed by auxiliary beta subunits of calcium-activated potassium channels. *Nat. Struct. Biol.* 10:448–454. http://dx.doi.org/10.1038/nsb932

Zhou, Y., X.M. Xia, and C.J. Lingle. 2011. Cysteine scanning and modification reveal major differences between BK channels and Kv channels in the inner pore region. *Proc. Natl. Acad. Sci. USA.* 108:12161–12166. http://dx.doi.org/10.1073/pnas.1104150108